Polymer 50 (2009) 4564–4570

Contents lists available at ScienceDirect

Polymer

journal homepage: www.elsevier.com/locate/polymer

The influence of side chains on solubility and photovoltaic performance of dithiophene–thienopyrazine small band gap copolymers

Arjan P. Zoombelt [a,b], Mark A.M. Leenen [a], Marta Fonrodona [a,b], Yohann Nicolas [a,b], Martijn M. Wienk [a], René A.J. Janssen [a,*]

[a] Molecular Materials and Nanosystems, Eindhoven University of Technology, P.O. Box 513, 5600 MB Eindhoven, The Netherlands
[b] Dutch Polymer Institute (DPI), P.O. Box 902, 5600 AX Eindhoven, The Netherlands

ARTICLE INFO

Article history:
Received 18 April 2009
Received in revised form
15 July 2009
Accepted 16 July 2009
Available online 22 July 2009

Keywords:
Polymer synthesis
Polymer composite materials
Photovoltaics

ABSTRACT

Three small band gap copolymers based on alternating dithiophene and thienopyrazine units were synthesized via Yamamoto coupling and applied in bulk heterojunction solar cells as donor together with PCBM ([6,6]-phenyl C_{61} butyric acid methyl ester) as acceptor. The polymers have an optical band gap of about 1.3 eV in the solid state and only vary by the chemical nature of the solubilizing side chains. The nature of the side chain has a major effect on solubility and processability of the polymer. Using *n*-butoxymethyl side chains a soluble, easy to process polymer was obtained that gave the best photovoltaic performance. With short-circuit currents up to 5.2 mA/cm^2 an efficiency of 0.8% was achieved under estimated standard solar light conditions (AM1.5G, 100 mW/cm^2) with spectral response up to 950 nm.

1. Introduction

In recent years, many small band gap polymers have been synthesized and applied in bulk heterojunction solar cells [1–11]. The most widely used strategy to obtain small band gap polymers involves the alternation of electron-rich and electron-deficient units along the polymer chain. These *p*-type semiconducting polymers are designed to absorb a large part of the solar spectrum and with *n*-type materials like methanofullerenes (i.e. the [6,6]-phenyl C_{61} and C_{71} butyric acid methyl esters; [60]PCBM and [70]PCBM) have already provided solar cells with power conversion efficiencies that approach 6% [7,9,11]. Judicious positioning of the energy levels of the polymer with respect to those of the fullerene acceptor is crucial for the ultimate photovoltaic performance. The highest occupied molecular orbital (HOMO) and lowest unoccupied molecular orbital (LUMO) of the polymer determine the optical band gap and thereby the fraction of solar photons absorbed and the maximum photocurrent. To ensure quantitative electron transfer to the acceptor, it is has been suggested that the LUMO of the polymer must be 0.3–0.4 eV above the LUMO of the acceptor [12,13]. However, raising the HOMO and LUMO levels of the polymer with respect to the levels of the acceptor, reduces the open-circuit voltage (V_{oc}) that is governed by the energy difference between the HOMO of the donor and the LUMO of the acceptor [14,15]. Following these rules, a successful small band gap polymer combines a low lying HOMO for high voltage and a high-lying LUMO level for good electron transfer, and therefore needs a carefully optimized compromise to maintain a small band gap.

When designing polymers for bulk heterojunction solar cells, solubility is an important parameter. Solubilizing side chains are incorporated to allow the synthesis of monomers and high molecular weight polymers. While side chains do not absorb light or transport charges, and do not contribute to the photocurrent, they generally strongly influence the morphology and charge carrier mobility. Bulky substituents may reduce or even prevent three-dimensional ordering of the polymer in the solid state. Generally, replacing linear alkyl side chains by branched chains reduces charge carrier mobility by preventing close packing and crystallinity, and therefore possibly lowers photovoltaic performance [16–20]. It is thus preferred to keep the amount of bulky side chains to minimum, but still ensure adequate solubility to enable obtaining high molecular weight polymers that are beneficial for obtaining efficient solar cells [21,22] and can be solution processed.

Here we report the synthesis and photovoltaic performance of three small band gap copolymers comprising alternating dithiophene and thienopyrazine units (Fig. 1). Incorporation of these units in an alternating fashion results in a reduction of the band gap [1,23–27], and we explore the use of different side chains to tune the solubility and photovoltaic properties. PBOTT contains four linear octyl side chains per repeat unit, while in PBEHTT the two octyl chains on the pyrazine ring are replaced by branched 2-ethyl-

* Corresponding author. Tel.: +31 40 2473597; fax: +31 40 2451036.
E-mail address: r.a.j.janssen@tue.nl (R.A.J. Janssen).

0032-3861/$ – see front matter © 2009 Elsevier Ltd. All rights reserved.
doi:10.1016/j.polymer.2009.07.028

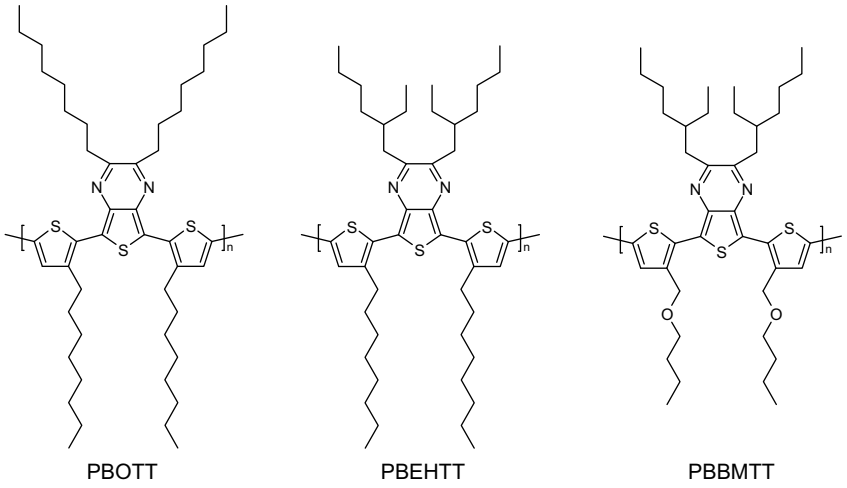

Fig. 1. Structure of PBOTT, PBEHTT and PBBMTT.

hexyl chains to increase solubility. In PBBMTT also the octyl side chains on the thiophene rings are replaced. The *n*-butoxymethyl chains used in PBBMTT are known to substantially enhance solubility and also increase the oxidation potential of the polymer via an inductive effect, that may increase V_{oc} [28,29].

2. Experimental section

The synthetic procedures for preparing monomer and polymers, and their characterization by ^{1}H and ^{13}C NMR are described in detail in Supporting Information. Molecular weights were determined using size exclusion chromatography in HPLC-grade *o*-dichlorobenzene (ODCB) at 80 °C against polystyrene standards on a Polymer Laboratories-GPC 120 high temperature chromatograph, a PD 2040 high temperature light scattering detector, and a Midas autosampler. A mixed-C 300 × 7.5 mm column was used, together with a pre-column. The flow rate was 1 ml/min and the injection volume was 100 μl.

UV–vis absorption spectra were measured with a Perkin–Elmer Lambda 900 spectrometer. Cyclic voltammetry (scan rate = 100 mV/s) was performed on an Autolab PGSTAT30 potentiostat in a three-electrode single-compartment cell using ODCB containing 0.1 M $TBAPF_6$ (Fluka) as electrolyte. The working electrode was platinum disk, the counter electrode a silver rod, and the reference electrode Ag/AgCl. Potentials are relative to Fc/Fc^{+} as internal standard.

Photovoltaic devices were made by spin coating PEDOT:PSS (Baytron P, VP Al 4083, HC Starck) onto pre-cleaned, patterned indium tin oxide (ITO) substrates (14 Ω per square). The photoactive layer was deposited by spin coating from the appropriate

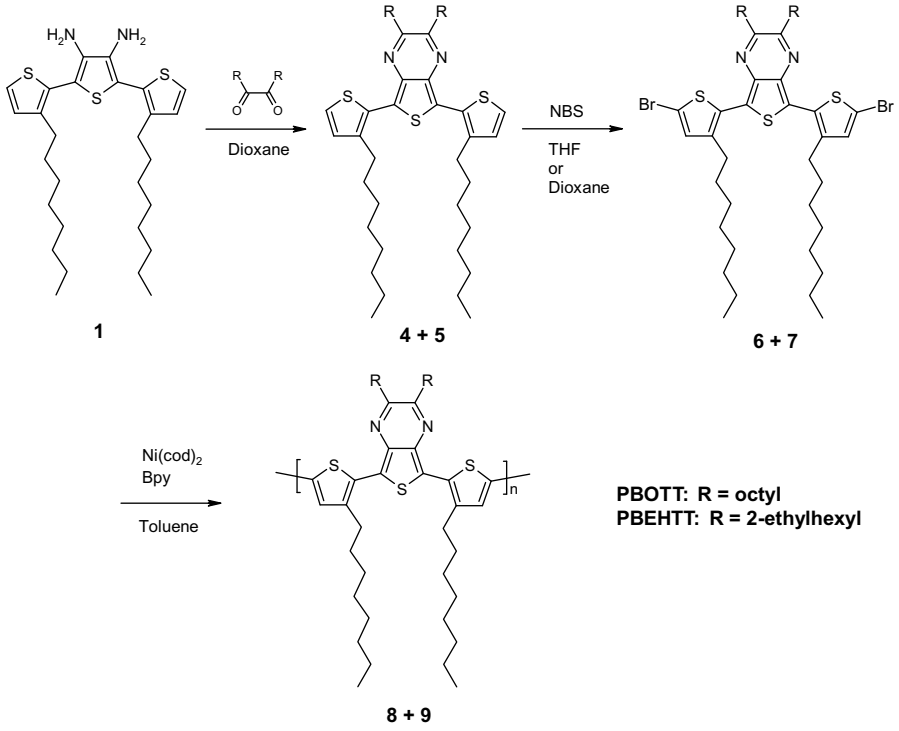

Scheme 1. Synthetic route towards PBOTT (**8**) and PBEHTT (**9**).

solvent. The counter electrode of LiF (1 nm) and aluminum (100 nm) was deposited by vacuum evaporation at 5×10^{-6} mbar. The active area of the cells was 0.17 cm^2. Monochromatic spectral response was measured on devices kept behind a quartz window in a nitrogen filled container with a Keithley 2400 source meter, using light from a tungsten halogen lamp, dispersed by an Oriel Cornerstone 130 monochromator. A calibrated Si cell was used as reference. The light intensity difference is determined from J_{sc} under monochromatic light and the estimated J_{sc} under AM1.5G. *J–V* characteristics were measured under ~110 mW/cm^2 white light from a tungsten halogen lamp filtered using Schott GG385 UV filter and a 300 nm ITO on glass near-IR filter, using a Keithley 2400 source meter. The J_{sc} obtained from the *J–V* curves is an overestimate due to the spectral mismatch and relatively high intensity (110 mW/cm^2) of the tungsten halogen lamp compared to the solar spectrum. Short-circuit currents under standard solar illumination conditions (J_{sc}(SR)) were obtained from convolution of the spectral response with the AM1.5G (100 mW/cm^2) solar spectrum. The estimated power conversion efficiency was determined by combining J_{sc}(SR) with V_{oc} and FF from the *J–V* measurements. We have reported previously that, for similar devices, this procedure affords estimated conversion efficiencies that are virtually identical to those obtained with a solar simulator and correcting for spectral mismatch [8].

Tapping Mode AFM was measured in a NanoScope Dimension 3100 microscope (Veeco, Digital Instruments) using PPP-NCHR probes (Nanosensors).

3. Results and discussion

3.1. Synthesis

The synthesis route towards PBOTT and PBEHTT is depicted in Scheme 1. Starting from 3,3″-dioctyl-[2,2′;5′,2″]terthiophene-3′,4′-diamine (**1**) [26], condensation coupling with either octadecane-7,8-dione (**3**) or 5,10-diethyltetradecane-7,8-dione (**2**) yielded the monomers (**4**, **5**). A subsequent bromination, by applying 2 equivalents of *N*-bromosuccinimide (NBS) in THF or dioxane, allows polymerization via Yamamoto coupling using bis(1,5-cyclooctadiene)nickel(0) (Ni(cod)$_2$) in toluene. The molecular weights (M_w) of these green polymers, determined by high temperature GPC in ODCB, were $M_w = 60$ kg/mol with PDI = 3.3 for **8** and $M_w = 36$ kg/mol PDI = 2.6 for **9**.

The synthesis of PBBMTT is outlined in Scheme 2. Starting from 3-thiophenemethanol, a Williamson-ether synthesis using 1-bromobutane followed by a bromination using NBS leads to the formation of 2-bromo-3-(*n*-butoxymethyl)thiophene (**11**) in good yield. Synthesis of stannane **12** allowed a Stille cross coupling reaction with 2,5-dibromo-3,4-dinitrothiophene giving terthiophene **13**. After reducing the nitro groups with iron dust in acetic acid, condensation of the diamine with 5,10-diethyltetradecane-7,8-dione (**2**) afforded monomer (**14**). Adding 2 equivalents of NBS to **14** in THF gave **15**, which was polymerized via Yamamoto coupling employing Ni(cod)$_2$ and resulted in a green polymer (**16**) with $M_w = 130$ kg/mol and PDI = 3.3.

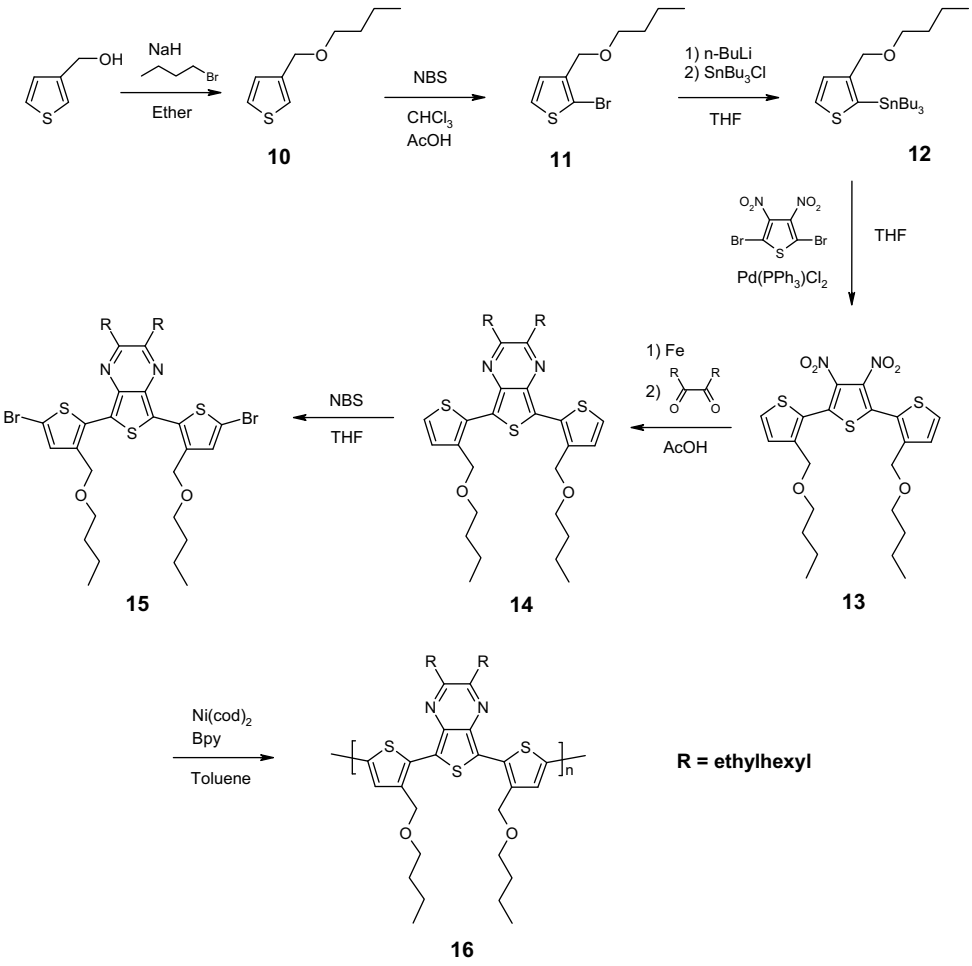

Scheme 2. Synthetic route towards PBBMTT (**16**).

3.2. Optical properties

The optical absorption spectra of the polymers in ODCB solution are shown in Fig. 2. The optical band gaps as determined from the onset of absorption range from 1.3 eV for PBOTT and PBEHTT to almost 1.5 eV for PBBMTT. At this concentration and temperature PBEHTT and PBOTT are partly aggregated in solution which leads to a red shift of the absorption via interchain delocalization. This red shift is most pronounced for PBOTT, which is the least soluble. At elevated temperatures both PBOTT and PBEHTT are more dissolved. Above 50 °C (Fig. 3b) the spectrum of PBEHTT no longer shows the characteristic aggregate absorption in the 750–950 nm range and seems to be molecularly dissolved. However, PBOTT still exhibits a small shoulder at 850–950 nm at 100 °C in ODCB, indicating that even at these high temperatures it is not fully molecularly dissolved (Fig. 3a). We note that this high tendency to partly aggregate may result in an apparent increase of the molecular weight and polydispersity determined by GPC in ODCB at 80 °C.

Although at room temperature PBBMTT shows a small shoulder at about 860 nm, aggregation is virtually absent. Apparently, despite the much higher molecular weight, the *n*-butoxymethyl side chains in PBBMTT reduce aggregation and greatly enhance solubility, consistent with previous results for poly(3-(*n*-butoxymethyl)-thiophene) [28]. In fact, the enhanced solubility is a likely cause for the substantially higher molecular weight obtained for this polymer.

The optical band gap in thin solid films of ~1.3 eV is identical for all polymers (Fig. 4). Whereas the spectra of PBOTT and PBEHTT show only small changes going from solution (room temperature) to film, PBBMTT exhibits a significant bathochromic shift. Apparently, incorporating a *n*-butoxymethyl side chain increases solubility but does not prevent a close packing in solid state. The prospect of having a better soluble polymer that still shows 3D order in film, while keeping the number of side chains to a minimum, is very appealing and of importance when designing and synthesizing new polymers for bulk heterojunction solar cells. Solubility is a prerequisite for processing and synthesis, whereas high three-dimensional order is considered to be beneficial for absorption and charge carrier mobility.

3.3. Electrochemistry

The oxidation and reduction potentials of the polymers were determined by cyclic voltammetry (CV) in ODCB and the results are listed in Table 1. The electrochemical band gap is determined as the difference between the onsets of the reduction and oxidation potential ($E_g^{cv} = E_{onset}^{ox} - E_{onset}^{red}$). The reduction potential is identical for the three polymers within the accuracy of the measurement but the oxidation potentials differ more. The constant reduction potential points to a more localized LUMO on the thienopyrazine units in the polymer chain [30,31]. The fact that the oxidation potential of PBBMTT is somewhat higher than that of PBEHTT is consistent with

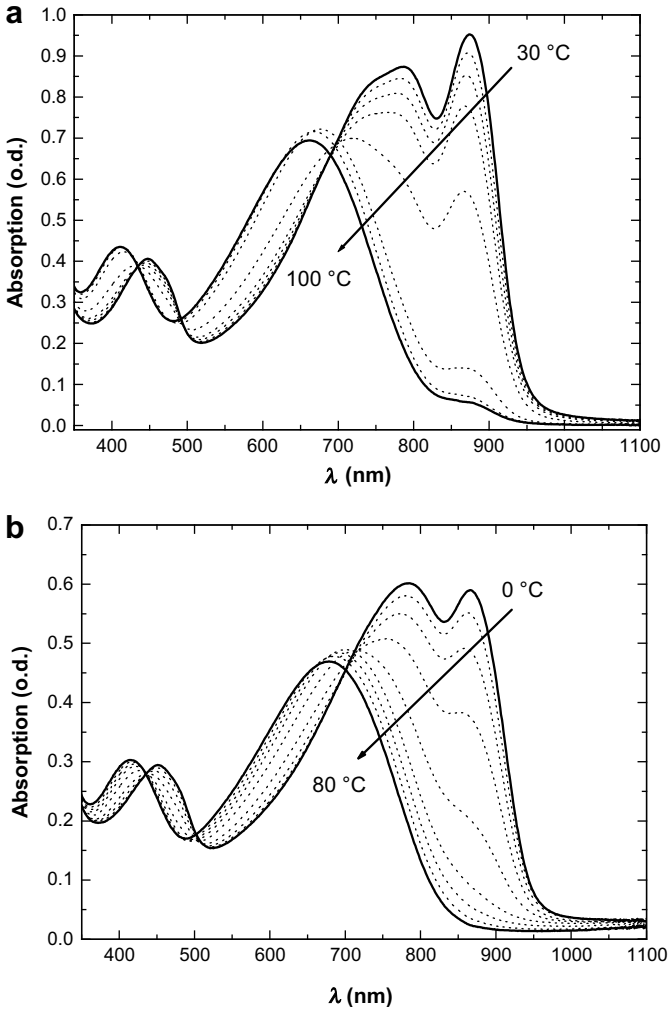

Fig. 3. Temperature dependent absorption of PBOTT (a) and PBEHTT (b) in ODCB recorded in 10 °C intervals.

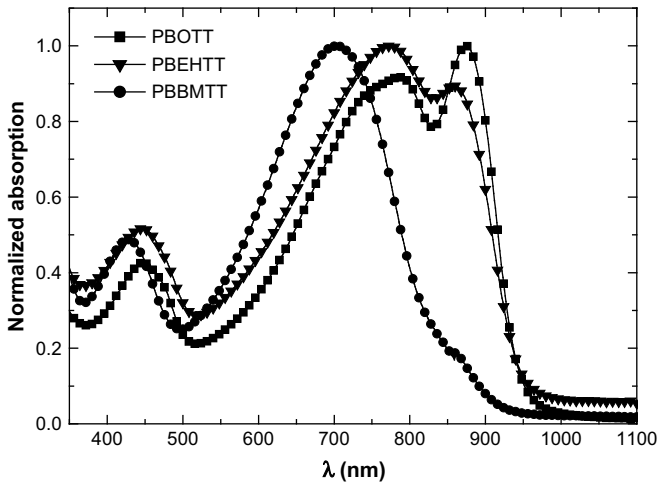

Fig. 2. Room temperature UV–vis absorption spectra of the polymers in OBCB solution.

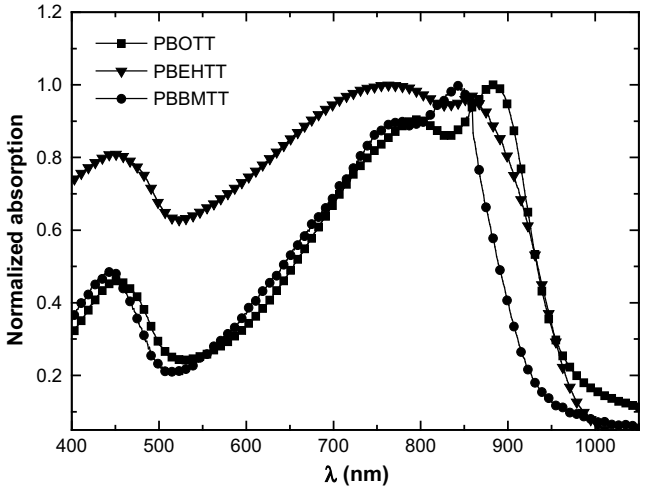

Fig. 4. UV–vis absorption spectra of the polymers in solid state.

Table 1
Optical and electrochemical data of the polymers in ODCB and in thin films.

Polymer	Solution							Film		
	λ_{max} (nm)	λ_{onset} (nm)	E_g (eV)	ε (L/g cm)	E^{ox}_{onset} (V)	E^{red}_{onset} (V)	E^{cv}_g (eV)	λ_{max} (nm)	λ_{onset} (nm)	E_g (eV)
PBOTT	874	942	1.32	34	−0.17	−1.78	1.61	882	965	1.28
PBEHTT	776	942	1.32	24	−0.29	−1.80	1.51	857	945	1.31
PBBMTT	702	840	1.48	37[a]	−0.26	−1.79	1.53	841	929	1.33

Electrochemical potentials (vs. Fc/Fc^+) in ODCB containing 0.1 M $TBAPF_6$ (scan rate = 100 mV/s, concentration 2×10^{-3} M based on monomer units).
[a] Determined in $CHCl_3$.

the replacement of the octyl side chains by the inductive electron-withdrawing *n*-butoxymethyl groups that can increase the oxidation potential by up to 30 mV [28,29]. The oxidation potential of PBOTT deviates substantially exhibiting a E^{ox}_{onset} of −0.17 V (Table 1). This is rather unexpected since its chemical structure is identical to that of PBEHTT. However, the reduced solubility of PBOTT compared to PBEHTT may cause that only the shorter oligomers are molecularly dissolved and therefore electroactive in the cyclic voltammetry experiment. In fact, the oxidation potential of −0.17 V corresponds well to values reported earlier for similar oligomers [31]. This also explains the discrepancy between electrochemical and optical band gaps. At concentrations at which absorption is measured, aggregated polymer determines the onset of absorption and thus the optical band gap. These aggregated species are not detected with CV, hence only redox potentials of molecularly dissolved polymer is obtained. When the onset of the absorption of the molecular dissolved polymer chains is used (Figs. 2 and 3), the optical band gaps are 1.49 (±0.02) eV, much closer to the electrochemical gaps.

The oxidation potentials of these polymers are relatively low and although no oxidation was observed in our experiments, their long-term stability under ambient conditions maybe limited [32].

3.4. Solar cells

The polymers were applied as electron donor in bulk heterojunction solar cells with [60]PCBM as electron acceptor. The active layers were spin coated onto an indium tin oxide (ITO) covered glass substrate, covered by a 60 nm film of PEDOT:PSS. After deposition of the active layer, 1 nm LiF and 100 nm Al were thermally evaporated as back electrode. Generally, the polymer:PCBM mixtures were spin coated in a ratio 1:4 (by wt.) from either chlorobenzene (CB), ODCB, or chloroform ($CHCl_3$), with a polymer concentration of 5 mg/ml.

The optimal photovoltaic parameters for each polymer are shown in Table 2. The limited solubility of PBOTT made processing very difficult, especially to attain good quality films of the PBOTT:[60]PCBM blend. The mixture had to be spin coated from ODCB at 150 °C onto hot substrates, which made reproducibility very challenging. The best device gave $V_{oc} = 0.29$ V and a fill factor FF = 0.50 (Fig. 5a) under white light illumination (110 mW/cm^2). The relatively low V_{oc} is consistent with the low oxidation potential of PBOTT [14,15]. The EQE is about 10% over the entire wavelength range up to 950 nm (Fig. 5b). Convolution of the spectral response (SR) (Fig. 5b) with the AM1.5G spectrum afforded an estimate of $J_{sc}(SR) = 4.5$ mA/cm^2 under standard solar light conditions (AM1.5G, 100 mW/cm^2), providing an estimated energy conversion efficiency of $\eta = 0.7\%$.

Table 2
Photovoltaic performance of PBOTT, PBEHTT and PBBMTT with [60]PCBM.

Polymer	Solvent	Layer thickness (nm)	V_{oc} (V)	$J_{sc}(SR)$ (mA/cm^2)	FF (-)	η(%)
PBOTT	ODCB	n.d.	0.29	4.5	0.50	0.7
PBEHTT	CB	130	0.39	3.0	0.45	0.5
PBBMTT	CB	108	0.43	5.2	0.37	0.8

The enhanced solubility of PBEHTT simplified processing considerably and PBEHTT:[60]PCBM blends could be spin coated from various solvents at room temperature (see Supporting Information). Spin coating from CB gave the highest efficiency cells with $V_{oc} = 0.39$ V, FF = 0.45, and $J_{sc}(SR) = 3.0$ mA/cm^2 (i.e. from the spectral response), resulting in $\eta = 0.5\%$. Although PBEHTT is much better processable and provides a higher V_{oc}, the overall performance is inferior to that of PBOTT due to a significantly lower current. In spectral response (Fig. 5b) it is clear that in the 650–950 nm range, external quantum efficiencies are significantly lower.

For PBBMTT solubility and processability were further enhanced due to the *n*-butoxymethyl side chains. The V_{oc} of solar cells made with PBBMTT:[60]PCBM as active layer, spin coated from CB, was

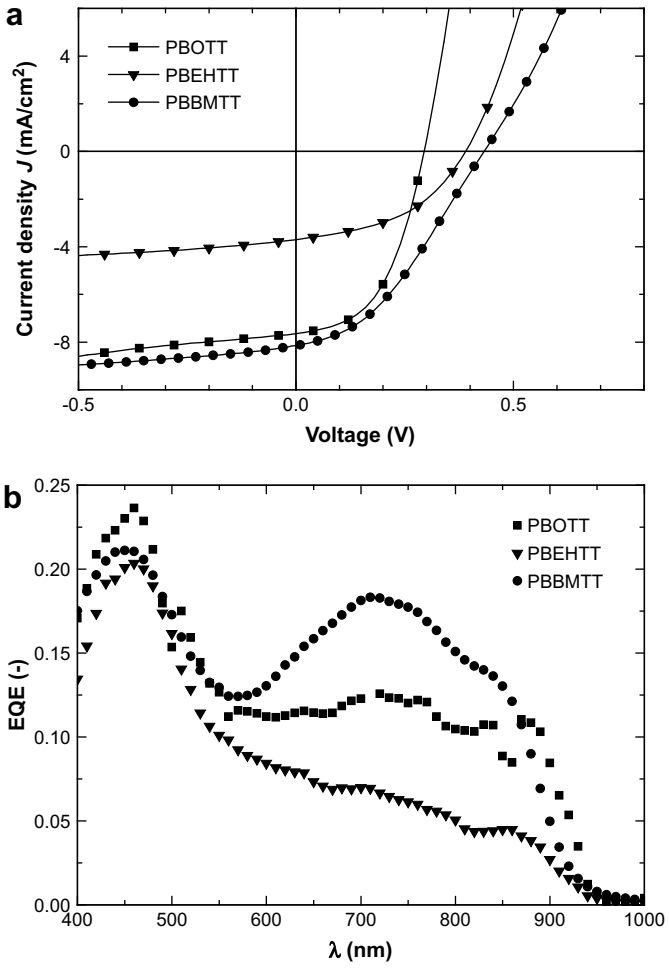

Fig. 5. (a) *J–V* curves of polymer:[60]PCBM solar cells under white light illumination from a tungsten halogen. (b) Monochromatic EQE of polymer:[60]PCBM solar cells.

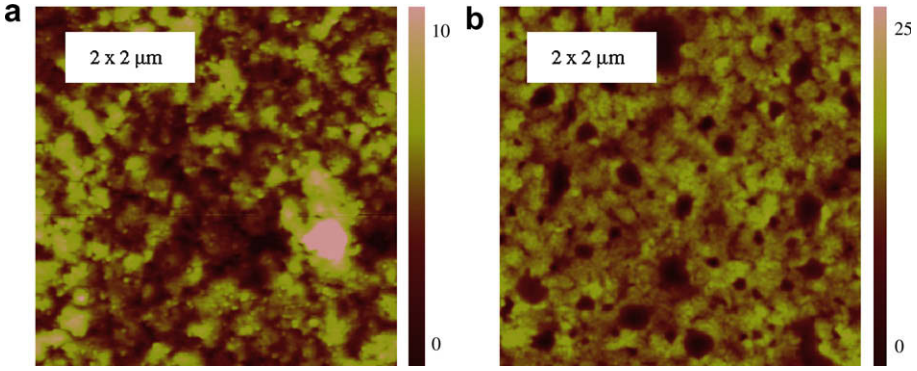

Fig. 6. AFM height images of [60]PCBM blended with (a) PBEHTT and (b) PBBMTT, both spin coated from CB.

found to be slightly better with 0.43 V. This increase, although small, is similar to the difference in oxidation potential between the polymers. The short-circuit current improved up to $J_{sc}(SR) = 5.2$ mA/cm^2 and the EQE well exceeds 15% in the 400–500 nm and in the 650–850 nm ranges. A relatively low fill factor of 0.37 limits the estimated power conversion efficiency to 0.8%.

Furthermore, we note that the contribution from the aggregated polymer (at ~850 nm) in the spectral response does not correspond to its absorption intensity in the pristine polymer film (Fig. 4). This can be explained by the reduced tendency for polymer chains to order and aggregate in mixtures with PCBM [33] and is reflected in a larger contribution from the non-aggregated chains at 650–750 nm.

3.5. Morphology

The key idea in bulk heterojunction solar cells is to obtain an intimately mixed active layer with a nanoscopic phase separation to ensure quantitative charge dissociation at the donor–acceptor interface [34–39]. Subsequently, percolating pathways allow efficient transport of the created charge carriers to their corresponding electrodes. It is thus important to study and optimize the active layer morphology, since it may lead to an enhanced photovoltaic performance. Atomic Force Microscopy (AFM) reveals the topography of the blend and gives generally a good first insight into morphology of the active layer [36]. Fig. 6 shows the AFM height images of PBEHTT:[60]PCBM and PBBMTT:[60]PCBM layers, spin coated from CB. Both films are rather uniform and do display features in the size of several tens of nanometers and a significant roughness. The tendency of the polymer and PCBM to aggregate or crystallize can lead to such phase segregation at the top surface and can often be changed by changing the processing solvent. However, the use of other solvents did not improve photovoltaic performance for either of the two blends (see Supporting Information). For example, using ODCB resulted in really smooth and homogeneous films of PBEHTT:[60]PCBM which produced a much lower current. Insufficient percolating pathways or increased recombination probably limit charge transport. Spin coating PBBMTT:[60]PCBM from $CHCl_3$ gave a very large phase separation but caused the current to drop significantly, possibly due to a reduced number of excitons that reach the interface [40]. The fill factor, however, did go up indicating that the charges that are created can efficiently reach the electrodes.

The poor solubility of PBOTT made it very difficult to obtain good reproducible films when spin coating PBOTT:[60]PCBM from ODCB at 150 °C. An optical image (see Figure S4 in Supporting Information) of the substrate clearly shows the poor film quality. No AFM images of these devices were recorded.

4. Conclusions

Three small band gap dithiophene–thienopyrazine copolymers with different solubilizing side chains were synthesized via a Yamamoto polymerization reaction. The nature of the side chain strongly influences the molecular weight obtained in the reaction and the solubility of the final polymer. The highest molecular weight ($M_w = 130$ kg/mol) was obtained for PBBMTT that comprises branched 2-ethylhexyl and *n*-butoxymethyl side chains. In contrast to PBBMTT, PBOTT and PBEHTT, with linear octyl chains on the thiophene rings, readily aggregate at room temperature in ODCB as evidenced from a red-shifted aggregate absorption peak. In thin films the optical band gap of the three polymers is virtually identical (~1.3 eV). This demonstrates that also the more soluble PBBMTT can form interchain aggregates in the solid state. Blended with [60]PCBM as an acceptor, each of the polymers can be processed into a working photovoltaic cell with spectral response covering UV, visible and near-IR up to 950 nm. The best devices were obtained for more soluble polymers. In a solar cell PBBMTT:[60]PCBM layers gave $V_{oc} = 0.43$ V, FF = 0.37, and an estimated $J_{sc} = 5.2$ mA/cm^2 under AM1.5G conditions, reaching an efficiency of $\eta = 0.8\%$. For the other two polymers the overall performance was less (0.7 and 0.5%). The correlation between molecular structure and solar cell parameters (V_{oc}, J_{sc}, FF, and η, Table 2) does not show clear trends. The three polymers have the same conjugated backbone and differ only in the nature of the side chains (linear/branched/ether function). This makes that differences in performance are not directly due to electronic effects but rather to differences in e.g. molecular weight, solubility, tendency to aggregate and morphology. This study shows that introducing *n*-butoxymethyl side chains increases solubility (which enhances processabiliy and leads to higher molecular weights in the synthesis) but does not prevent aggregation (which enhances charge transport and leads to a red shift of the absorption) and hence results in improved performance. This property makes these side chains very interesting candidates for use in π-conjugated polymers for bulk heterojunction solar cells.

Acknowledgement

This work is part of the research program of the Dutch Polymer Institute (DPI, projects 325 and 524).

Appendix. Supplementary data

Supplementary data associated with this article can be found in the online version, at doi:10.1016/j.polymer.2009.07.028

References

[1] Campos LM, Tontcheva A, Guenes S, Sonmez G, Neugebauer H, Sariciftci NS, et al. Chem Mater 2005;17:4031–3.
[2] Dhanabalan A, Van Duren JKJ, Van Hal PA, Van Dongen JLJ, Janssen RAJ. Adv Funct Mater 2001;11:255–62.
[3] Wang X, Perzon E, Delgado JL, De la Cruz P, Zhang F, Langa F, et al. Appl Phys Lett 2004;85:5081–3.
[4] Inganäs O, Svensson M, Zhang F, Gadisa A, Persson NK, Wang X, et al. Appl Phys A 2004;79:31–5.
[5] Zhang F, Mammo W, Andersson LM, Admassie S, Andersson MR, Inganäs O. Adv Mater 2006;18:2169–73.
[6] Mühlbacher D, Scharber M, Morana M, Zhu Z, Waller D, Gaudiana R, et al. Adv Mater 2006;18:2884–9.
[7] Peet J, Kim JY, Coates NE, Ma WL, Moses D, Heeger AJ, et al. Nature Mater 2007;6:497–500.
[8] Wienk MM, Turbiez M, Gilot J, Janssen RAJ. Adv Mater 2008;20:2556–60.
[9] Hou J, Chen HY, Zhang S, Li G, Yang Y. J Am Chem Soc 2008;130:16144–5.
[10] Zhou E, Nakamura M, Nishizawa T, Zhang Y, Wei Q, Tajima K, et al. Macromolecules 2008;41:8302–5.
[11] Liang Y, Wu Y, Feng D, Tsai ST, Son HJ, Li G, et al. J Am Chem Soc 2009;131:56–7.
[12] Scharber MC, Mühlbacher D, Koppe M, Denk P, Waldauf C, Heeger AJ, et al. Adv Mater 2006;18:789–94.
[13] Koster LJA, Mihailetchi VD, Blom PWM. Appl Phys Lett 2006;88:093511/1–093511/3.
[14] Gadisa A, Svensson M, Andersson MR, Inganäs O. Appl Phys Lett 2004;84:1609–11.
[15] Brabec CJ, Cravino A, Meissner D, Sariciftci NS, Fromherz T, Rispens MT, et al. Adv Funct Mater 2001;11:374–80.
[16] McCulloch I, Heeney M, Bailey C, Genevicius K, MacDonald I, Shkunov M, et al. Nature Mater 2006;5:328–33.
[17] Chabinyc ML, Toney MF, Kline RJ, McCulloch I, Heeney M. J Am Chem Soc 2007;129:3226–37.
[18] Hwang IW, Cho S, Kim JY, Lee K, Coates NE, Moses D, et al. J Appl Phys 2008;104:033706/1–033706/9.
[19] Morana M, Wegscheider M, Bonanni A, Kopidakis N, Shaheen S, Scharber M, et al. Adv Funct Mater 2008;18:1757–66.
[20] Zhang M, Tsao HN, Pisula W, Yang C, Mishra AK, Müllen K. J Am Chem Soc 2007;129:3472–3.
[21] Schilinsky P, Asawapirom U, Scherf U, Biele M, Brabec CJ. Chem Mater 2005;17:2175–80.
[22] Peet J, Cho NS, Lee SK, Bazan GC. Macromolecules 2008;41:8655–9.
[23] Wienk MM, Turbiez MGR, Struijk MP, Fonrodona M, Janssen RAJ. Appl Phys Lett 2006;88:153511/1–153511/3.
[24] Zhu Y, Champion RD, Jenekhe SA. Macromolecules 2006;39:8712–9.
[25] Petersen MH, Hagemann O, Nielsen KT, Jorgensen M, Krebs FC. Sol Energy Mater Sol Cells 2007;91:996–1009.
[26] Kitamura C, Tanaka S, Yamashita Y. J Chem Soc Chem Comm 1994:1585–6.
[27] Karsten BP, Janssen RAJ. Org Lett 2008;10:3513–6.
[28] Zoombelt AP, Leenen MAM, Fonrodona M, Wienk MM, Janssen RAJ. Thin Solid Films 2008;516:7176–80.
[29] Roncali J, Garreau R, Delabouglise D, Garnier F, Lemaire M. Synth Met 1989;28:C341–8.
[30] Salzner U, Koese ME. J Phys Chem B 2002;106:9221–6.
[31] Karsten BP, Viani L, Gierschner J, Cornil J, Janssen RAJ. J Phys Chem A 2008;112:10764–73.
[32] De Leeuw DM, Simenon MMJ, Brown AR, Einerhand REF. Synth Met 1997;87:53–9.
[33] Cremer J, Wienk MM, Janssen RAJ, Bäuerle P. Chem Mater 2006;18:5832–4.
[34] Van Duren JKJ, Yang X, Loos J, Bulle-Lieuwma CWT, Sieval AB, Hummelen JC, et al. Adv Funct Mater 2004;14:425–34.
[35] Hoppe H, Sariciftci NS. J Mater Chem 2006;16:45–61.
[36] Yang X, Loos J. Macromolecules 2007;40:1353–62.
[37] Hoppe H, Niggemann M, Winder C, Kraut J, Hiesgen R, Hinsch A, et al. Adv Funct Mater 2004;14:1005–11.
[38] Liu J, Shi Y, Yang Y. Adv Funct Mater 2001;11:420–4.
[39] Gebeyehu D, Brabec CJ, Padinger F, Fromherz T, Hummelen JC, Badt D, et al. Synth Met 2001;118:1–9.
[40] Wienk MM, Kroon JM, Verhees WJH, Knol J, Hummelen JC, van Hal PA, et al. Angew Chem Int Ed 2003;42:3371–5.